

Stiffness analysis for a 3-PUU parallel kinematic machine

Yangmin Li ^{*}, Qingsong Xu

*Department of Electromechanical Engineering, Faculty of Science and Technology, University of Macau,
Av. Padre Tomás Pereira S.J., Taipa, Macao*

Received 15 November 2005; received in revised form 20 April 2006; accepted 7 February 2007
Available online 6 April 2007

Abstract

This paper presents the stiffness characteristics of a three-prismatic-universal–universal (3-PUU) translational parallel kinematic machine (PKM). The stiffness matrix is derived intuitively based upon an alternative approach considering actuations and constraints, and the compliances subject to both actuators and legs are involved in the stiffness model. The stiffness performance of the manipulator is evaluated by utilizing the extremum stiffness values, and the influences of design parameters on the stiffness properties are presented, which will be valuable for the architecture design of a 3-PUU PKM. Moreover, the stiffness behavior of the PKM is investigated via the eigenscrew decomposition of the stiffness matrix, which provides a physical interpretation of the PKM stiffness and allows the identification of the stiffness center and compliant axis.

© 2007 Elsevier Ltd. All rights reserved.

Keywords: Parallel manipulators; Stiffness; Analysis; Workspace; Mechanism design

1. Introduction

In recent years, parallel manipulators have been investigated and developed more and more widely for various applications [1]. At the same time, less-DOF (degree-of-freedom) parallel manipulators with less than six DOF have been applied extensively in many situations since they both maintain the inherent advantages of parallel mechanisms and possess several other merits in terms of the total cost reduction in manufacturing and operations [2–4].

Stiffness is one of the most important performances of parallel mechanisms, particularly for those which are used as machine tools, because higher stiffness allows higher machining speeds with higher accuracy of the end-effector. Therefore, it is quite necessary to perform the stiffness modeling and to evaluate a parallel kinematic machine (PKM) in the early design stage. The three-prismatic-universal–universal (3-PUU) translational parallel mechanism was proposed and investigated before [5,6]. However, there are no efforts made towards the assessment of its stiffness considering the compliances in both the actuators and legs. The stiffness

^{*} Corresponding author. Tel.: +853 3974464; fax: +853 28838314.
E-mail address: yqli@umac.mo (Y. Li).

model of a 3-PUU PKM is derived in this paper, which is firstly used to evaluate its stiffness over the workspace in order to see the effect of altering the kinematic parameters in the structure and then further utilized to have a physical view of the PKM compliant behavior.

1.1. Stiffness modeling

Regarding a rigid body elastically suspended by elastic devices, if only small displacements from its unpreloaded equilibrium position are considered, the overall spatial force–deflection relation of the mechanism is linear, which is described by a 6×6 symmetric positive semidefinite matrix [7], i.e., the stiffness matrix. Generally, the stiffness characteristics of a parallel manipulator can be described by the 6×6 stiffness matrix, which relates the vector of compliant deformations of the end-effector to an external static wrench that is applied on the manipulator [8]. By taking into account the flexibilities of every compliant elements, the stiffness model of 6-DOF parallel manipulators with six legs can be established straightforwardly [9]. While for those less-DOF parallel manipulators, it is not easy to derive their overall stiffness matrices. For instance, the stiffness of a tripod-based PKM is modeled in [10] by decomposing the whole machine structure into two separate substructures, and formulating the stiffness model of each substructure by means of virtual work principle. A stiffness model of the 3-DOF CaPaMan parallel manipulator is established in [11] by taking into account the kinematic and static features of the three legs in view of the motions of every joint and link.

An observation of the stiffness modeling of less-DOF parallel manipulators reveals that it is not obvious what is the best way since the existing approaches are not intuitive enough. In this paper, a new approach is presented to directly derive the stiffness matrix of a less-DOF parallel manipulator based upon an overall Jacobian which is previously proposed in [12] to identify both the architecture and constraint singularities. Via this approach, a 6×6 stiffness matrix that is defined as the overall stiffness matrix including the stiffness of actuators and constraints of a less-DOF parallel manipulator can be established intuitively, which is shown by the stiffness modeling of a 3-PUU translational PKM in this paper.

1.2. Stiffness evaluation

For a given PKM, the stiffness changes with the variation of the manipulator configurations within its workspace as well as the direction of the applied wrenches. Once the stiffness model is derived, it is desired to predict its stiffness characteristics over the workspace in order to assess whether the design is satisfied with the stiffness requirements or even further to perform an optimal design with the stiffness considered especially in the design stage. Moreover, it is necessary to investigate the stiffness behavior of a PKM at specified configurations to have an insight into its stiffness behavior.

As far as the approaches for stiffness evaluation are concerned, several different performance indices have been proposed and utilized in the literatures. A simple way to predict the stiffness is to use the interested stiffness factors, i.e., the terms of the stiffness matrix [8,10]. Besides, the stiffness can be evaluated using the eigenvalue of the stiffness matrix which is experienced in the direction of the corresponding eigenvector [8,13]. It has been shown that the stiffness is bounded by the minimum and maximum eigenvalues of the stiffness matrix [14]. Based on this point, the stiffness values have been predicted by the minimum, maximum, and average eigenvalues, even magnitude of the ratio of the maximum and minimum eigenvalues of the stiffness matrix [14]. Additionally, the determinant of stiffness matrix, which is the product of its eigenvalues, has been adopted to assess the stiffness of parallel manipulators [5,11]. Furthermore, similar to the condition number of Jacobian matrix, the condition number of the stiffness matrix has been introduced, then a global stiffness index defined as the inverse of the condition number of the stiffness matrix integrated over the reachable workspace and divided by the workspace volume is presented to assess the stiffness of a 3-DOF spherical parallel manipulator [15].

Among these usually used stiffness performance indices, the stiffness factor is preferred to be applied to evaluate the stiffness matrix only with a diagonal form. Because for a stiffness matrix with the generic form, the off-diagonal terms couple the forces/torques applied in the corresponding directions, it follows that individual stiffness factors cannot totally reflect the stiffness property in any directions. Concerning the determinant or trace of the stiffness matrix, it cannot distinguish the situations in which the manipulator has a very

low stiffness in one direction while a very high stiffness in another one, that leads to a high value of the determinant or trace although the low stiffness prohibits applying the manipulator for machine tool applications. Consequently, neither the determinant nor the trace of the stiffness matrix is a good choice for the stiffness evaluation of PKMs. And the same problem arises for the average of the eigenvalues of the stiffness matrix. In view of the condition number of the stiffness matrix, it indicates the ill-conditioning of the stiffness matrix, while does not provide enough information of the stiffness values. For the machine tool application, the minimum stiffness over the workspace should be larger than a specified value to ensure the accuracy of the manipulation everywhere in the workspace. Hence, the minimum and maximum values of stiffness and their variances appear to be the reasonable indices for stiffness evaluation, and are adopted as stiffness performance indices in this paper.

In addition, once the stiffness model of a PKM is established, it is also desired to have a better understanding of the spatial compliant behavior of the PKM. It has been shown that the eigenscrew decomposition of the stiffness matrix can identify the basic structure of the stiffness and provide a physical interpretation of the spatial elastic behavior [7,16,17], then the center of stiffness and the compliant axis [18] can also be identified if they exist. The center of stiffness is a generalization of the RCC (remote center of compliance) concept, at which the stiffness matrix can be expressed as a normal form with the off-diagonal blocks diagonalized. Although the normal form itself obtained for generic stiffness matrices is not diagonal, it still maximally decouples rotational and translational aspects of stiffness. Moreover, the compliant axis is a useful concept for robotic applications, since it acts as independent torsional and linear springs. For a compliant axis, a force produces a parallel linear deformation, and a rotational deformation about the line of the force produces a parallel couple.

In the remainder of this paper, after a brief description of the 3-PUU PKM in Section 2, the procedure for the stiffness matrix determination using an alternative approach is presented in Section 3. Then in Section 4, the stiffness is evaluated by adopting the minimum and maximum stiffness as performance indices, and the influences of design parameters on the stiffness characteristics are predicted. Moreover, the stiffness behaviors of the PKM are evaluated based upon the eigenscrew decomposition of the stiffness matrix along with the stiffness center and compliant axis identified. Finally, some concluding remarks are presented in Section 5.

2. Kinematic description

The CAD model of a 3-PUU PKM is shown in Fig. 1 and the schematic diagram is described by Fig. 2. The manipulator consists of a mobile platform, a fixed base, and three limbs with identical kinematic structure. Each limb connects the fixed base to the moving platform by a prismatic (P) joint followed by two universal (U) joints in sequence, where the P joint is driven by a lead screw linear actuator.

Since each U joint consists of two intersecting revolute (R) joints, each limb is kinematically equivalent to a PRRRR kinematic chain. A 3-PUU mechanism can be arranged to achieve only translational motions with

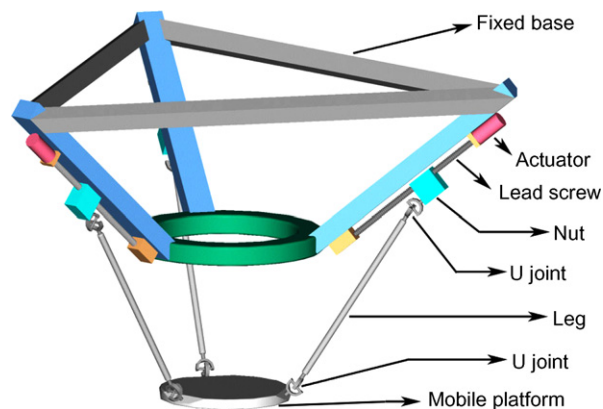


Fig. 1. A 3-PUU PKM.

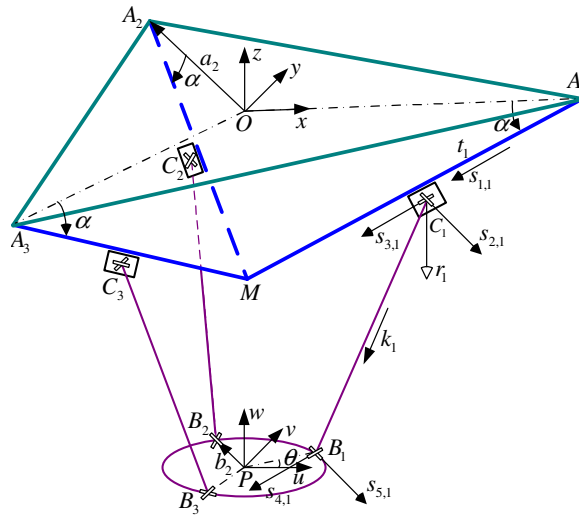


Fig. 2. Schematic representation of a 3-PUU PKM.

some certain geometric conditions satisfied, i.e., in each kinematic chain, the axis of the first revolute joint is parallel to that of the last one, and the two intermediate joint axes are parallel to each other.

For the purpose of analysis, as depicted in Fig. 2, we assign a fixed Cartesian reference frame $O\{x, y, z\}$ at the centered point O of the fixed base platform $\Delta A_1A_2A_3$, and a moving frame $P\{u, v, w\}$ on the mobile platform at the centered point P of triangle $\Delta B_1B_2B_3$. In addition, let the x - and u -axes be parallel to each other, and the x -axis direct along \vec{OA}_1 . The angle between vectors \vec{OA}_i and \vec{PB}_i ($i = 1, 2, 3$) is defined as the twist angle θ , i.e., the angle between the mobile platform and the fixed base. The three rails A_iM intersect one another at point M , and intersect the x - y plane at points A_1, A_2 , and A_3 , that lie on a circle of radius a . The three legs C_iB_i with lengths of l intersect the u - v plane at points B_1, B_2 , and B_3 , which lie on a circle of radius b . In addition, angle α is measured from the fixed base to rails A_iM and is defined as the actuators layout angle. In order to achieve a symmetric workspace of the manipulator, both $\Delta A_1A_2A_3$ and $\Delta B_1B_2B_3$ are assigned to be equilateral triangles.

Let \mathbf{k}_i be an unit vector along the leg C_iB_i , d_i represent a linear displacement of the i th actuator, and \mathbf{h}_i denote the corresponding unit vector pointing along rail A_iM . In addition, let $\mathbf{a}_i = \vec{OA}_i$, $\mathbf{b}_i = \vec{PB}_i$, and $\mathbf{p} = \vec{OP} = [x \ y \ z]^T$. Using a suitable vector-loop analysis, both the inverse and forward kinematics problems can be solved in closed-forms. We recall briefly the inverse kinematics solutions as follows (see [6] for more details), which are used to determine the reachable workspace of the 3-PUU PKM

$$d_i = \mathbf{h}_i^T \mathbf{e}_i - \sqrt{(\mathbf{h}_i^T \mathbf{e}_i)^2 - \mathbf{e}_i^T \mathbf{e}_i + l^2}, \tag{1}$$

where $\mathbf{e}_i = \mathbf{p} + \mathbf{b}_i - \mathbf{a}_i$ for $i = 1, 2$, and 3 .

3. Stiffness matrix generation

3.1. Jacobian matrix derivation

The theory of reciprocal screws is an effective way to derive the Jacobian matrix of a parallel manipulator [12]. With \mathbf{v} and $\boldsymbol{\omega}$ respectively denoting the vectors for the linear and angular velocities, the twist of the mobile platform can be defined as $\mathbf{T} = [\mathbf{v}^T \ \boldsymbol{\omega}^T]^T$ in Plücker axis coordinate. Concerning a 3-PUU PKM, the connectivity of each limb is equal to 5, hence the instantaneous twist \mathbf{T} of the mobile platform can be expressed as a linear combination of the five instantaneous twists, i.e.,

$$\mathbf{T} = \dot{d}_i \hat{\mathbf{T}}_{1,i} + \dot{\theta}_{2,i} \hat{\mathbf{T}}_{2,i} + \dot{\theta}_{3,i} \hat{\mathbf{T}}_{3,i} + \dot{\theta}_{4,i} \hat{\mathbf{T}}_{4,i} + \dot{\theta}_{5,i} \hat{\mathbf{T}}_{5,i} \tag{2}$$

for $i = 1, 2, 3$, where $\dot{\theta}_{j,i}$ is the intensity and $\hat{\mathbf{T}}_{j,i}$ denotes an unit screw (in Plücker axis coordinate) associated with the j th joint of the i th limb, and

$$\hat{\mathbf{T}}_{1,i} = \begin{bmatrix} \mathbf{s}_{1,i} \\ \mathbf{0} \end{bmatrix}, \quad \hat{\mathbf{T}}_{2,i} = \begin{bmatrix} \mathbf{c}_i \times \mathbf{s}_{2,i} \\ \mathbf{s}_{2,i} \end{bmatrix}, \quad \hat{\mathbf{T}}_{3,i} = \begin{bmatrix} \mathbf{c}_i \times \mathbf{s}_{3,i} \\ \mathbf{s}_{3,i} \end{bmatrix}, \quad \hat{\mathbf{T}}_{4,i} = \begin{bmatrix} \mathbf{b}_i \times \mathbf{s}_{4,i} \\ \mathbf{s}_{4,i} \end{bmatrix}, \quad \hat{\mathbf{T}}_{5,i} = \begin{bmatrix} \mathbf{b}_i \times \mathbf{s}_{5,i} \\ \mathbf{s}_{5,i} \end{bmatrix}$$

can be identified, with $\mathbf{s}_{j,i}$ represents an unit vector along the j th joint axis of the i th limb, $\mathbf{c}_i = \mathbf{b}_i - l\mathbf{k}_i$, and $\mathbf{0}$ denotes a 3×1 zero vector. In addition, as a translational PKM, the joint axes of the 3-PUU mechanism are assembled to satisfy the conditions: $\mathbf{s}_{3,i} = \mathbf{s}_{4,i}$ and $\mathbf{s}_{2,i} = \mathbf{s}_{5,i}$.

Firstly, one screw $\hat{\mathbf{t}}_{c,i}$ expressed in Plücker ray coordinate that is reciprocal to all the joint screws of the i th limb forms a 1-system, which can be identified as an infinite pitch screw with a direction perpendicular to the two joint axes of a U joint, i.e.,

$$\hat{\mathbf{t}}_{c,i} = \begin{bmatrix} \mathbf{0} \\ \mathbf{r}_i \end{bmatrix}, \tag{3}$$

where \mathbf{r}_i is an unit vector along the direction defined by $\mathbf{s}_{2,i} \times \mathbf{s}_{3,i}$ (or $\mathbf{s}_{5,i} \times \mathbf{s}_{4,i}$).

Taking the product of both sides of Eq. (2) with $\hat{\mathbf{t}}_{c,i}$, leads to three equations, which can be assembled into the matrix form:

$$\mathbf{J}_c \mathbf{T} = \mathbf{0}, \tag{4}$$

where

$$\mathbf{J}_c = \begin{bmatrix} \mathbf{0} & \mathbf{r}_1^T \\ \mathbf{0} & \mathbf{r}_2^T \\ \mathbf{0} & \mathbf{r}_3^T \end{bmatrix}_{3 \times 6} \tag{5}$$

is called the Jacobian of constraints. Each row in \mathbf{J}_c denotes an unit wrench of constraints imposed by the joints of a limb, the combination of which constrains the mobile platform a 3-DOF motion. Hence, if \mathbf{r}_i for $i = 1, 2, 3$ are linearly independent, the unique solution to Eq. (4) is $\boldsymbol{\omega} = \mathbf{0}$.

Secondly, with the actuators locked, the reciprocal screws of each limb form a 2-system which includes the screw $\hat{\mathbf{t}}_{c,i}$ identified earlier. One additional basis screw $\hat{\mathbf{t}}_{a,i}$ being reciprocal to all the passive joint screws of the i th limb can be identified as a zero pitch screw along the direction passing through the two U joints, i.e.,

$$\hat{\mathbf{t}}_{a,i} = \begin{bmatrix} \mathbf{k}_i \\ \mathbf{b}_i \times \mathbf{k}_i \end{bmatrix}. \tag{6}$$

Similarly, taking the product of both sides of Eq. (2) with $\hat{\mathbf{t}}_{a,i}$, leads to a matrix-form result:

$$\mathbf{J}_a \mathbf{T} = \dot{\mathbf{q}}, \tag{7}$$

where $\dot{\mathbf{q}} = [\dot{d}_1 \ \dot{d}_2 \ \dot{d}_3]^T$ denotes the actuated joint rate and

$$\mathbf{J}_a = \begin{bmatrix} \mathbf{k}_1^T & (\mathbf{b}_1 \times \mathbf{k}_1)^T \\ \mathbf{k}_1^T \mathbf{s}_{1,1} & \mathbf{k}_1^T \mathbf{s}_{1,1} \\ \mathbf{k}_2^T & (\mathbf{b}_2 \times \mathbf{k}_2)^T \\ \mathbf{k}_2^T \mathbf{s}_{1,2} & \mathbf{k}_2^T \mathbf{s}_{1,2} \\ \mathbf{k}_3^T & (\mathbf{b}_3 \times \mathbf{k}_3)^T \\ \mathbf{k}_3^T \mathbf{s}_{1,3} & \mathbf{k}_3^T \mathbf{s}_{1,3} \end{bmatrix}_{3 \times 6} \tag{8}$$

is called the Jacobian of actuations.

An observation of the units of matrix \mathbf{J}_a reveals that the first three columns are dimensionless while the last three ones are related to the units of length which are introduced by the position vectors \mathbf{b}_i . As shown in the following discussions, the matrices \mathbf{J}_a and \mathbf{J}_c are integrated into the overall stiffness matrix of the manipulator, thus it is necessary to homogenize the units of the Jacobian matrices so as to generate a stiffness matrix and performance index invariant of the length unit adopted. Since \mathbf{J}_c is dimensionless, the dimensionally homogeneous Jacobian of actuations can be achieved by

$$\mathbf{J}_{ah} = \mathbf{J}_a \mathbf{W} \tag{9}$$

with $\mathbf{W} = \text{diag}[1, 1, 1, \frac{1}{b}, \frac{1}{b}, \frac{1}{b}]$, where the mobile platform radius b is chosen as the characteristic length to homogenize the dimension of the Jacobian matrix.

Combining Eqs. (4) and (7) allows the generation of

$$\dot{\mathbf{q}}_0 = \mathbf{J} \mathbf{T}, \tag{10}$$

where $\dot{\mathbf{q}}_0 = [\dot{d}_1 \ \dot{d}_2 \ \dot{d}_3 \ 0 \ 0 \ 0]^T$ is the extended joint rate, and

$$\mathbf{J} = \begin{bmatrix} \mathbf{J}_{ah} \\ \mathbf{J}_c \end{bmatrix}_{6 \times 6} \tag{11}$$

is called the overall Jacobian of a 3-PUU PKM, which is homogeneous in terms of units.

3.2. Stiffness modeling

It can be observed that the wrench system that is the infinite pitch reciprocal screw system of constraints exerts three constraint couples to the mobile platform, and the wrench system which is the zero pitch reciprocal screw system of actuations imposes three constraint forces to the mobile platform with the directions along the legs. This means that each leg suffers a force and a couple along the leg's direction. With the assumption that the rigidities of the U joints and mobile platform are infinite, the compliance subject to actuators and legs can be derived as follows.

3.2.1. Compliance subject to actuators

In a lead screw actuation system, through the torque transmission, the force acting on the i th nut and the corresponding linear displacement can be respectively calculated as

$$f_i = \frac{2\tau_i}{\mu_c d_s} \quad \text{and} \quad \Delta t_i = \frac{p\tau_i}{K_{\alpha,i}}, \tag{12}$$

where μ_c is the friction coefficient, τ_i and $K_{\alpha,i}$ denote the torque and torsional stiffness of the i th actuator, d_s and p represent the pitch diameter and lead of the lead screw, respectively.

In view of Eq. (12), one can derive the compliance for the i th linear driving device:

$$C_i = \frac{\Delta t_i}{f_i} = \frac{\mu_c d_s p}{2K_{\alpha,i}}. \tag{13}$$

Hence, the projection of compliance subject to the i th actuator in the corresponding leg's direction can be derived as

$$C_{\alpha,i}^k = \mathbf{k}_i^T \mathbf{s}_{1,i} C_i. \tag{14}$$

3.2.2. Compliance subject to legs

Let $C_{l,i}^k$ and $C_{\theta,i}^k$ be the longitudinal and transverse compliance of the i th leg. Since each leg suffers a constraint force (F_i^k) along the leg's direction and a constraint couple (M_i^r) with its direction perpendicular to the universal joint of the limb, the elastic deformations of the i th leg due to the force and couple can be expressed as

$$\Delta l_i = C_{l,i}^k F_i^k = \frac{l}{AE} F_i^k, \tag{15}$$

$$\Delta \theta_i = C_{\theta,i}^k M_i^r = \frac{l}{GI_p} \mathbf{k}_i^T \mathbf{r}_i M_i^r, \tag{16}$$

where l and A denote the length and cross section area of each leg, E and G are the moduli of the longitudinal and transverse elasticity, and I_p represents the polar moment of inertia, respectively.

Then, an observation of Eqs. (15) and (16) allows the generation of $C_{l,i}^k$ and $C_{\theta,i}^k$.

3.2.3. Stiffness model

In view of the inverse relationship between the stiffness and compliance, the stiffness of actuators and constraints can be respectively obtained as

$$K_{a,i} = C_{a,i}^{-1} = (C_{a,i}^k + C_{l,i}^k)^{-1}, \tag{17a}$$

$$K_{c,i} = C_{c,i}^{-1} = (C_{\theta,i}^k)^{-1} \tag{17b}$$

for $i = 1, 2,$ and 3 .

In consequence, the stiffness model of a 3-PUU PKM can be established by considering that the mobile platform is connected to the fixed base by three linear springs and three rotational ones as illustrated in Fig. 3.

3.3. Stiffness matrix determination

Assume that the mobile platform suffers an external wrench $\mathbf{w} = [\mathbf{f}^T \ \mathbf{m}^T]^T$ expressed in the Plücker ray coordinate, where $\mathbf{f} = [f_x \ f_y \ f_z]^T$ denotes a force and $\mathbf{m} = [m_x \ m_y \ m_z]^T$ denotes a torque. Additionally, let τ_a and τ_c represent the reaction forces/torques of actuators and constraints, respectively. In the absence of gravity, the external wrench is balanced by the reaction forces/torques exerted by the actuators and constraints, i.e.,

$$\mathbf{w} = \mathbf{J}_a^T \tau_a + \mathbf{J}_c^T \tau_c, \tag{18}$$

where the reaction forces/moments can be expressed as

$$\tau_a = \boldsymbol{\chi}_a \Delta \mathbf{q}_a, \tag{19a}$$

$$\tau_c = \boldsymbol{\chi}_c \Delta \mathbf{q}_c \tag{19b}$$

with $\Delta \mathbf{q}_a$ and $\Delta \mathbf{q}_c$ denote the displacements of actuators and constraints, respectively, and the diagonal matrices are $\boldsymbol{\chi}_a = \text{diag}[K_{a,1}, K_{a,2}, K_{a,3}]$ and $\boldsymbol{\chi}_c = \text{diag}[K_{c,1}, K_{c,2}, K_{c,3}]$, respectively.

Moreover, let $\Delta \mathbf{x} = [\Delta x \ \Delta y \ \Delta z]^T$ and $\Delta \boldsymbol{\theta} = [\Delta \theta_x \ \Delta \theta_y \ \Delta \theta_z]^T$ be the infinitesimal displacements of translation and rotation of the mobile platform with respect to three axes of the reference frame. And then, applying the principle of virtual work by neglecting the gravitational effect, allows the generation of

$$\mathbf{w}^T \Delta \mathbf{X} = \tau_a^T \Delta \mathbf{q}_a + \tau_c^T \Delta \mathbf{q}_c, \tag{20}$$

where $\Delta \mathbf{X} = [\Delta \mathbf{x}^T \ \Delta \boldsymbol{\theta}^T]^T$ denotes the mobile platform’s twist deformation in the axis coordinate.

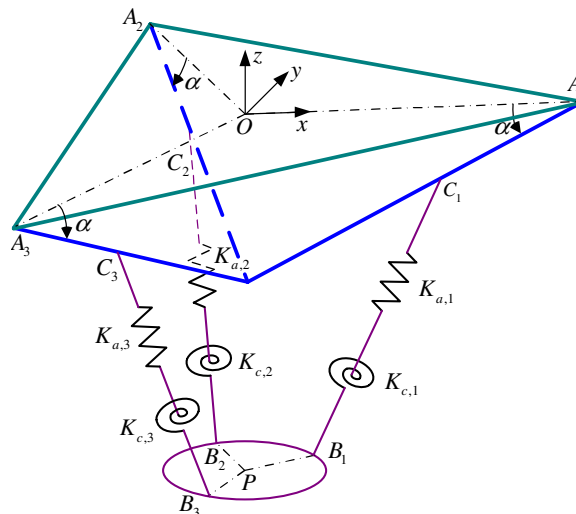


Fig. 3. Stiffness model of a 3-PUU PKM.

A careful analysis of Eqs. (18)–(20) at the same time, leads to the expression of

$$\mathbf{w} = \mathbf{K}\Delta\mathbf{X}, \tag{21}$$

where $\mathbf{K} = \mathbf{J}^T \boldsymbol{\chi} \mathbf{J}$ is defined as the 6×6 overall stiffness matrix of a 3-PUU PKM including the effect of actuations and constraints, with the 6×6 diagonal matrix $\boldsymbol{\chi} = \text{diag}[\boldsymbol{\chi}_a \ \boldsymbol{\chi}_c]$.

4. Stiffness evaluation of a 3-PUU PKM

The architectural parameters of a 3-PUU PKM are shown in Table 1, which are designed to make a compromise between the performance of global dexterity index over the entire workspace and the space utility ratio index defined as the ratio of total workspace volume to physical size of the robot [6]. In addition, the cone angle limits of the U joints are $\pm 20^\circ$ and the motion range limits of the P joints are assigned to be $\pm \Delta 0.1$ m. By adopting a numerical searching method described in [19], the reachable workspace of the manipulator is generated as shown in Fig. 4. Moreover, the physical parameters of the designed 3-PUU PKM are elaborated in Table 2.

Let the home position of the mobile platform be in the case of mid stroke of linear actuators, i.e., $d_i = 0$ ($i = 1, 2, 3$), in which the stiffness matrix can be calculated as follows:

Table 1
Architectural parameters of a 3-PUU PKM

Parameter	Value
a	0.3 m
b	0.1 m
l	0.3 m
α	45.0°
θ	0.0°

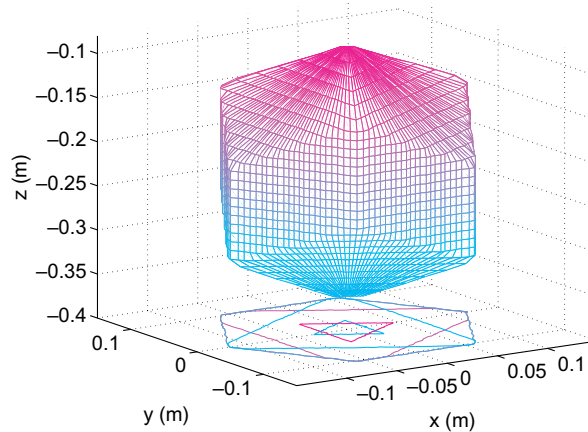


Fig. 4. Reachable workspace of a 3-PUU PKM.

Table 2
Physical parameters of a 3-PUU PKM

Parameter	Value	Parameter	Value
$K_{z,i}$	1.45×10^6 N m/rad	E	2.03×10^{11} N/m ²
μ_c	0.25	G	7.85×10^{10} N/m ²
d_s	20 mm	A	2.01×10^{-4} m ²
p	3 mm	I_p	3.22×10^{-9} m ⁴

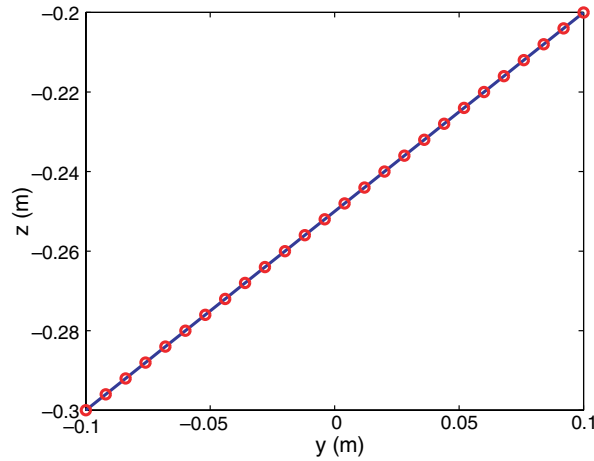


Fig. 5. Trajectory of the mobile platform in a plane of $x = 0$ m.

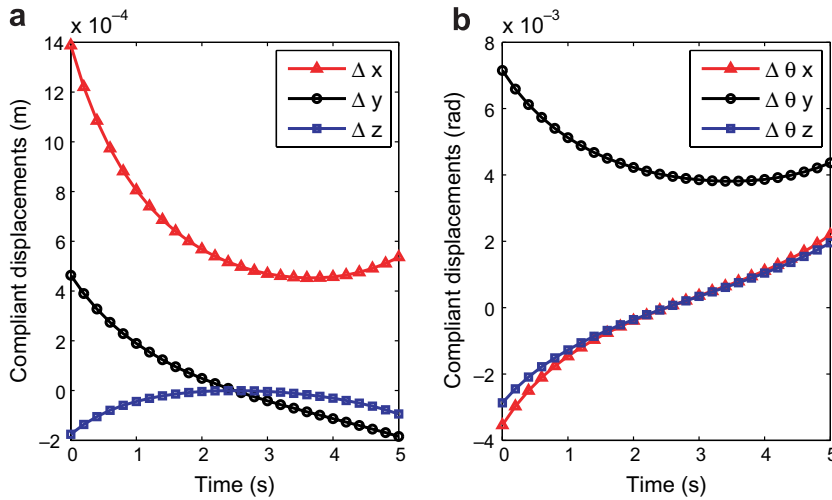


Fig. 6. The compliant displacements of (a) translations and (b) rotations of the mobile platform.

$$\mathbf{K}^0 = \begin{bmatrix} 9.0891 & 0 & 0 & 0 & -1.0162 & 0 \\ 0 & 9.0891 & 0 & 1.0162 & 0 & 0 \\ 0 & 0 & 22.7228 & 0 & 0 & 0 \\ 0 & 1.0162 & 0 & 0.1137 & 0 & 0 \\ -1.0162 & 0 & 0 & 0 & 0.1137 & 0 \\ 0 & 0 & 0 & 0 & 0 & 0.0001 \end{bmatrix} \times 10^7, \tag{22}$$

where the units of terms are N/m for $\{K_{11}^0, K_{22}^0, K_{33}^0\}$, N/rad for $\{K_{15}^0, K_{24}^0\}$, N m/m for $\{K_{42}^0, K_{51}^0\}$, and N/m/rad for $\{K_{44}^0, K_{55}^0, K_{66}^0\}$.

Given a wrench applied on the mobile platform of the PKM, the compliant displacements $\Delta \mathbf{X}$ can be derived in view of Eq. (21). Fig. 6 depicts the plots of compliant displacements when the mobile platform follows a trajectory shown in Fig. 5 at a constant velocity with an external static force of $f_x = 20$ N applied. It is observed that the maximum linear compliant displacement is 1.4 mm which occurs in the x -axis direction as expected. In addition, the maximum rotary compliant displacement is the rotation around the y -axis.

4.1. Stiffness assessment

In order to ensure the accuracy of the manipulation of the PKM anywhere in the workspace, the minimum stiffness over the workspace should be larger than a specified value. In this subsection, both the minimum and maximum eigenvalues obtained through the conventional eigenvalue decomposition of the stiffness matrix are used as stiffness indices so as to have a global view of the stiffness values over the workspace.

A numerical approach is adopted here to evaluate the stiffness throughout the PKM workspace. The main feature of the algorithm is the partition of a covering volume V in the Cartesian coordinate into small sampling pieces $\{v_i\}$ and the piece-by-piece check in order to recognize whether the piece v_i belongs to the workspace. The size of the samples is dependent on the required accuracy. The checking procedure is based upon the inverse kinematic solutions along with the consideration of motion limits of mechanical joints. In the pieces that fall into the workspace, the stiffness matrix is derived and decomposed to obtain the minimum and maximum stiffness, which are separately stored at the same time. Once the check of all the sampling pieces is completed, the stored minimum and maximum stiffness values are compared respectively to get the minimum and maximum values over the workspace.

The algorithm is adopted here due to the ease of implementation in a computer program. It should be noticed that other alternative approaches can also be adopted to the current problem, and one of them is the interval analysis algorithm, which has the advantages of allowing computer round-off errors to be taken into account and is applied to solve the complex forward kinematics of a Gough-type parallel manipulator successfully [20] and used for the design and comparison of two 3-DOF PKMs [3] and other problems.

The distributions for the minimum stiffness and maximum stiffness in the planes of $z = -0.224$ m (home position height) are illustrated in Fig. 7. It can be observed that, similar to the reachable workspace, the distribution of stiffness in a x - y plane is 120-deg-symmetrical about the axial directions of three P joints. In addition, the lowest value of minimum stiffness occurs around the boundary of the workspace, so does the highest value of the maximum stiffness, since the manipulator approaches singular when it comes near the workspace boundary.

Since around the boundary of the reachable workspace, the PKM takes on a bad stiffness property, it is reasonable to restrict the PKM to operate in a subworkspace located within the reachable workspace. According to the PKM tasks and performances, there are several ways to define this subworkspace. Here, for the main purpose of examining the effects of altering the kinematic parameters on the stiffness, the subworkspace is assigned as a cubic shape usable workspace with the edge length of 0.1 m, whose center lies at the home position point of the mobile platform. And the size of the sample pieces is chosen as 0.002 m for the numerical evaluation of the stiffness in the usable workspace.

Along with the varying of architectural parameters of the 3-PUU PKM, the tendency of variation on the minimum and maximum stiffness over the usable workspace is described in Figs. 8a–d, from which it is clear to

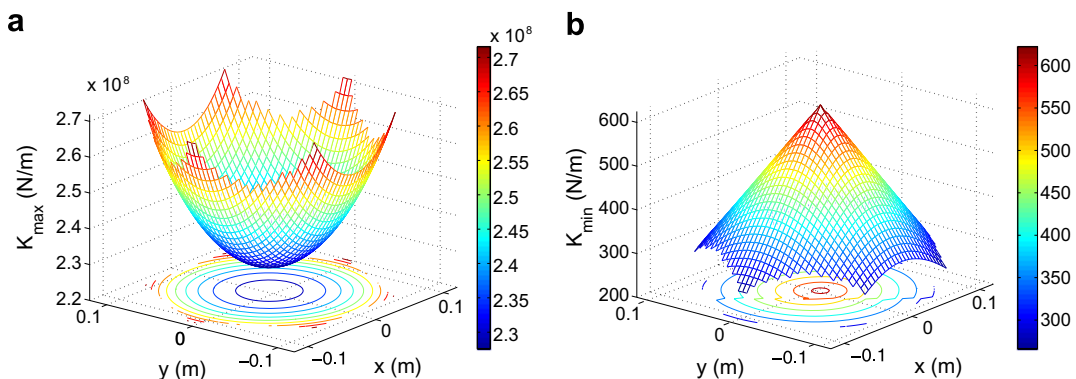


Fig. 7. The distribution for (a) minimum and (b) maximum stiffness in a plane of $z = -0.224$ m.

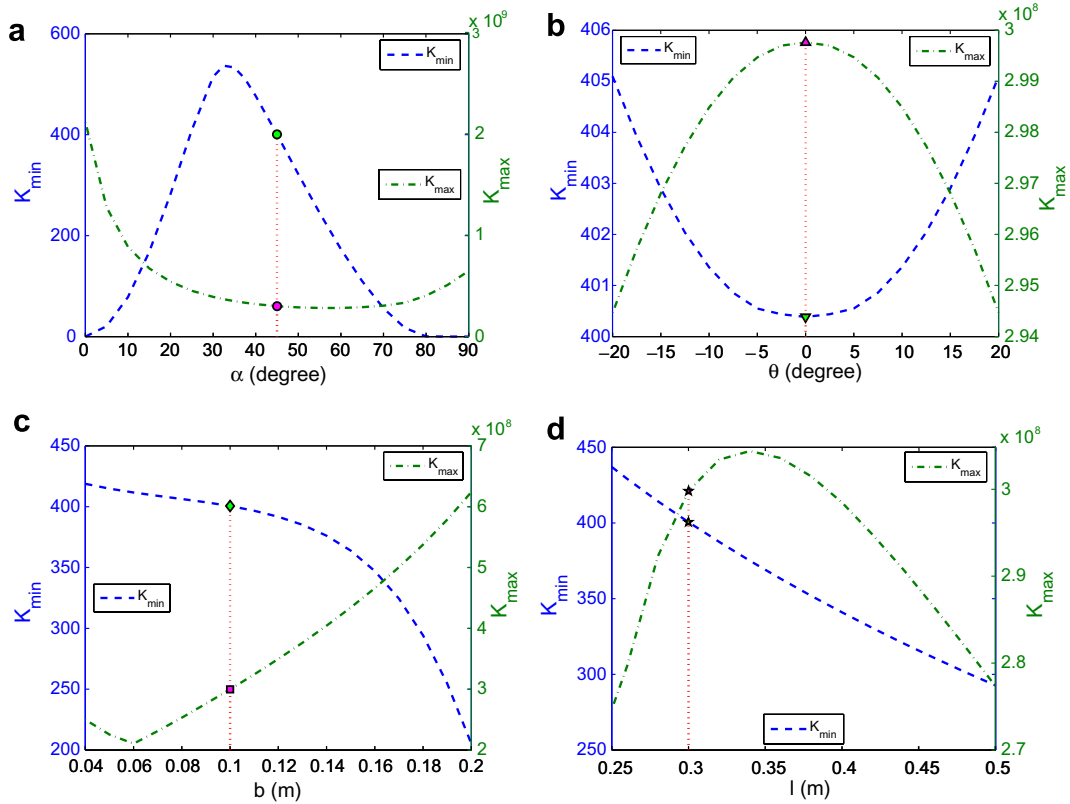


Fig. 8. Global stiffness index versus design parameters of (a) actuators layout angle, (b) twist angle, (c) mobile platform size, and (d) the leg length.

see the impacts of design parameters (α , θ , b , and l) on the stiffness property of the manipulator. For instance, along with the increasing of actuators layout angle α from 0° to 90° , the minimum stiffness seems to reach the highest value between 30° and 35° , and the maximum stiffness approaches the lowest value around 60° of actuators layout angle. Additionally, in case of the twist angle $\theta = 0^\circ$, the stiffness has a lowest minimum stiffness and a highest maximum stiffness values, and the minimum stiffness decreases monotonously as the increasing of the mobile platform size b from 0.05 m to 0.2 m and the leg length l from 0.25 m to 0.5 m, while in which ranges, there are extremum values for the maximum stiffness.

The stiffness indices for the manipulator with aforementioned parameters are also marked in Fig. 8. It is seen that the architectural parameters optimized for dexterity and workspace performances do not result in a manipulator with the highest minimum stiffness values. Since the objective of optimization depends heavily on the tasks to be performed, the stiffness indices provide a measure for the architectural optimization of the PKM particularly for machine tool applications.

4.2. Stiffness interpretation via eigenscrew decomposition

In what follows, the stiffness behavior is investigated through the eigenscrew decomposition of the stiffness matrix by resorting to useful results from previous relevant literatures.

In view of Plücker’s original conventions, a twist is expressed in the axis coordinate and a wrench is expressed in the ray coordinate. As far as the stiffness matrix eigenscrew problem is concerned, it should be formulated using consistent coordinates for the results to be meaningful. Either ray or axis screw coordinates can be utilized. In addition, this preserves the integrity of the units and ensures that the results are independent of the coordinate frame. Otherwise, the results are not invariant and thus become meaningless.

The conversion between the two types of coordinates is allowed by a matrix $\widehat{\Delta}$ with the expression of

$$\widehat{\Delta} = \begin{bmatrix} \mathbf{0} & \mathbf{I} \\ \mathbf{I} & \mathbf{0} \end{bmatrix}, \tag{23}$$

where $\mathbf{0}$ and \mathbf{I} denote a zero matrix and an identity matrix in 3×3 , respectively. The definition of $\widehat{\Delta}$ and a description of its characteristics are given in [16]. In general, $\widehat{\Delta}$ interchanges the first and last three components of a screw.

The eigenscrew problem formulated in the ray coordinate is described as follows:

$$\mathbf{K}\widehat{\Delta}\mathbf{e} = \lambda\mathbf{e}, \tag{24}$$

where the eigenvalue λ is defined as the eigenstiffness of the stiffness matrix \mathbf{K} , and the six-vector (screw) \mathbf{e} is defined as its corresponding eigenscrew of \mathbf{K} .

Based on Eq. (24), the eigenscrew decomposition of the stiffness matrix is stated in [17] as follows: Let \mathbf{K} be a full-rank stiffness matrix and \mathbf{w}_i be the unit eigenscrews corresponding to eigenstiffnesses λ_i ($i = 1, 2, \dots, 6$) obtained from the eigenscrew problem Eq. (24). Then \mathbf{K} can be decomposed into the form:

$$\mathbf{K} = \frac{\lambda_1}{2h_1}\mathbf{w}_1\mathbf{w}_1^T + \frac{\lambda_2}{2h_2}\mathbf{w}_2\mathbf{w}_2^T + \dots + \frac{\lambda_6}{2h_6}\mathbf{w}_6\mathbf{w}_6^T, \tag{25}$$

where

$$h_i = \frac{1}{2}\mathbf{w}_i^T\widehat{\Delta}\mathbf{w}_i \neq 0 \tag{26}$$

is the pitch of \mathbf{w}_i , for $i = 1, 2, \dots, 6$.

Let

$$k_i = \frac{\lambda_i}{2h_i}, \quad i = 1, \dots, 6, \tag{27}$$

then Eq. (25) indicates that \mathbf{K} can be interpreted by a body suspended by six screw springs each with spring wrench \mathbf{w}_i and spring constant k_i . The screw springs can be expressed as [7]

$$\mathbf{w}_i = \begin{bmatrix} \mathbf{n}_i \\ \mathbf{r}_i \times \mathbf{n}_i + h_i\mathbf{n}_i \end{bmatrix}, \tag{28}$$

where \mathbf{n}_i is an unit vector representing the direction of the spring axis, and \mathbf{r}_i identifies the direction and distance to the line of action.

The results from these previous investigations of the eigenscrew problem are used to study the stiffness behavior of the 3-PUU PKM. As an example, the eigenscrew decomposition is applied to the stiffness matrix \mathbf{K}^0 as described in Eq. (22). By solving the eigenscrew problem in Eq. (24), the six eigenstiffness $[\lambda]$, the six eigenscrew pitches $[h]$, and the six corresponding unit eigenscrews $[\mathbf{w}]$ obtained are detailed in Eq. (29).

$$\begin{aligned} [\lambda] &= \text{diag}[5.3631, -5.3631, 2.3984, -2.3984, 2.3984, -2.3984] \times 10^5, \\ [h] &= \text{diag}[0.0024, -0.0024, 0.0026, -0.0026, 0.0026, -0.0026], \\ [\mathbf{w}] &= \begin{bmatrix} 0 & 0 & 0.8801 & -0.8262 & -0.0236 & -0.0247 \\ 0 & 0 & 0.4749 & -0.5634 & -0.9997 & -0.9997 \\ 1 & 1 & 0 & 0 & 0 & 0 \\ 0 & 0 & 0.0554 & -0.0608 & -0.1118 & -0.1117 \\ 0 & 0 & -0.0971 & 0.0939 & 0 & 0.0054 \\ 0.0024 & -0.0024 & 0 & 0 & 0 & 0 \end{bmatrix}. \end{aligned} \tag{29}$$

The interpretation of stiffness matrix \mathbf{K}^0 based on eigenscrew decomposition is elaborated in Table 3, which indicates that \mathbf{K}^0 can be interpreted by a body suspended by six screw springs \mathbf{s}_i with directions along the eigenscrews of \mathbf{K}^0 as shown in Fig. 9. The pitch of helical joint (in length/rotation) used in the screw spring

Table 3
Spring constant and geometrical connection for each screw spring

Spring	$k \times 10^{-8}$	\mathbf{n}^T	\mathbf{r}^T	p
s_1	1.1361	[0, 0, 1]	[0, 0, 0]	-0.0148
s_2	1.1361	[0, 0, 1]	[0, 0, 0]	0.0148
s_3	0.4545	[0.8801, 0.4749, 0]	[0, 0, -0.1118]	-0.0166
s_4	0.4545	[-0.8262, -0.5634, 0]	[0, 0, -0.1118]	0.0166
s_5	0.4545	[-0.0236, -0.9997, 0]	[0, 0, -0.1118]	-0.0166
s_6	0.4545	[-0.0247, -0.9997, 0]	[0, 0, -0.1118]	0.0166

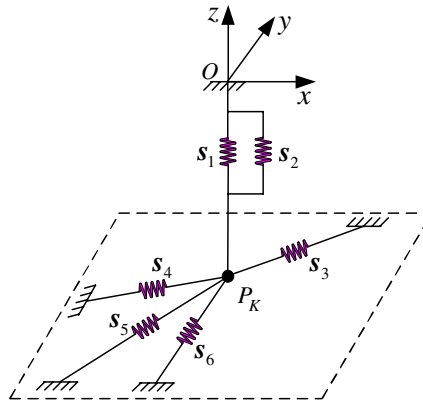


Fig. 9. The physical interpretation of the stiffness of a 3-PUU PKM.

is determined by $-2\pi h_i$. Thus, each screw spring is defined by its spring constant k , helical joint pitch p , and the geometrical connection parameters \mathbf{n} and \mathbf{r} . It can be observed that the first two springs are parallel to each other and along the z -axis, and the other four springs lie in a common plane perpendicular to the z -axis, i.e., the plane of $z = -0.1118$ m. Moreover, the six springs intersect at a common point $P_K(0, 0, -0.1118)$, that denotes the center of stiffness, at which the stiffness matrix can be brought to a normal form and allows the maximally decoupling of the rotations and translations.

4.3. Compliant axis determination

A compliant axis exists when a force produces a parallel linear deformation, and a rotational deformation about the line of the force produces a parallel couple [18]. The existence of a compliant axis is related to the corresponding eigenscrew problem. A necessary and sufficient condition for a compliant axis is that there are two collinear eigenscrews with eigenstiffnesses of equal magnitude and opposite sign. The compliant axis direction is determined by the direction of the two collinear eigenscrews.

In view of Eq. (29) and Table 3, it is observed that there exist two collinear eigenscrews in the direction of $[0, 0, 1]^T$, i.e., the z -axis direction, with the eigenstiffness of 5.3631×10^5 and -5.3631×10^5 , respectively. Therefore, there exists one compliant axis along the z -axis direction for the stiffness matrix \mathbf{K}^0 . A rotational deformation about the z -axis, according to Eq. (24), results in

$$\mathbf{K}^0 \hat{\Delta} [0 \ 0 \ 1 \ 0 \ 0 \ 0]^T = 10^3 [0 \ 0 \ 0 \ 0 \ 0 \ 1.2658]^T, \tag{30}$$

i.e., a pure couple parallel to the z -axis.

Taking the inverse of both sides of Eq. (24), yields

$$\hat{\Delta} \mathbf{K}^{-1} \mathbf{e} = \lambda^{-1} \mathbf{e}, \tag{31}$$

which represents the eigenscrew decomposition of the compliance matrix (\mathbf{K}^{-1}) actually. Applying a force along the z -axis, using Eq. (31), yields

$$\widehat{\Delta}(\mathbf{K}^0)^{-1}[0 \ 0 \ 1 \ 0 \ 0 \ 0]^T = 10^{-8}[0 \ 0 \ 0 \ 0 \ 0 \ 0.4401]^T, \quad (32)$$

i.e., a single linear deformation along the z -axis.

By examining any points on the z -axis, it is observed that when the mobile platform of the PKM lies in the z -axis, there always exist a compliant axis and a stiffness center in the z -axis direction. Therefore, from the accuracy point of view, the 3-PUU PKM has better operation in the z -axis, since the force and deformation about the compliant axis will not affect any other directions.

5. Conclusions

The stiffness matrix is derived based on an overall Jacobian via the theory of reciprocal screws considering the effect of actuations and constraints. And the rigidities in both actuators and legs are taken into account to establish the stiffness model of the manipulator. Through a survey of the commonly used stiffness performance indices, the minimum and maximum eigenvalues of the stiffness matrix over a cubic shape usable workspace are adopted to evaluate the stiffness of the PKM. The variation tendency of stiffness within the workspace is presented and the impact of variation of design parameters on the stiffness characteristics is given, that is helpful for the architecture design of a 3-PUU PKM considering stiffness performance. Furthermore, the eigenscrew decomposition of the stiffness matrix is carried out to have an insight view of the compliant behavior of the PKM stiffness. It is illustrated that, at a specified configuration, the stiffness can be interpreted by a body suspended by a set of screw springs. In addition, the PKM's stiffness is better along the z -axis since it always has a compliant axis and a stiffness center in that direction.

The main contribution of this paper lies in the derivation of the stiffness model of a 3-PUU PKM via an intuitive approach, the stiffness evaluation of the PKM with the variation of architectural parameters, and the physical interpretation of the PKM stiffness. Furthermore, the modeling and analysis methodology presented here can be generalized to other types of parallel manipulators as well. This paper provides a basis for the architectural design of the 3-PUU PKM with stiffness properties taken into account, which is necessary from the design point of view. Once a PKM is designed and fabricated, the experimental study will be performed to validate the results obtained from the stiffness analysis.

References

- [1] J.-P. Merlet, *Parallel Robots*, Kluwer Academic Publishers, London, 2000.
- [2] M. Carricato, V. Parenti-Castelli, A family of 3-DOF translational parallel manipulators, *ASME J. Mech. Des.* 125 (2) (2003) 302–307.
- [3] D. Chablat, P. Wenger, F. Majou, J.-P. Merlet, An interval analysis based study for the design and the comparison of three-degrees-of-freedom parallel kinematic machines, *Int. J. Robot. Res.* 23 (6) (2004) 615–624.
- [4] Y. Li, Q. Xu, Kinematic analysis and design of a new 3-DOF translational parallel manipulator, *ASME J. Mech. Des.* 128 (4) (2006) 729–737.
- [5] L.W. Tsai, S. Joshi, Kinematics analysis of 3-DOF position mechanisms for use in hybrid kinematic machines, *ASME J. Mech. Des.* 124 (2) (2002) 245–253.
- [6] Y. Li, Q. Xu, A new approach to the architecture optimization of a general 3-PUU translational parallel manipulator, *J. Intell. Robot. Syst.* 46 (1) (2006) 59–72.
- [7] S. Huang, J.M. Schimmels, Minimal realizations of spatial stiffnesses with parallel or serial mechanisms having concurrent axes, *J. Robot. Syst.* 18 (3) (2001) 135–146.
- [8] C. Gosselin, Stiffness mapping for parallel manipulators, *IEEE Trans. Robot. Automat.* 6 (3) (1990) 377–382.
- [9] N. Simaan, M. Shoham, Stiffness synthesis of a variable geometry six-degrees-of-freedom double planar parallel robot, *Int. J. Robot. Res.* 22 (9) (2003) 757–775.
- [10] T. Huang, X. Zhao, D.J. Whitehouse, Stiffness estimation of a tripod-based parallel kinematic machine, *IEEE Trans. Robot. Automat.* 18 (1) (2002) 50–58.
- [11] M. Ceccarelli, G. Carbone, A stiffness analysis for CaPaMan (Cassino Parallel Manipulator), *Mech. Mach. Theory* 37 (5) (2002) 427–439.
- [12] S.A. Joshi, L.W. Tsai, Jacobian analysis of limited-DOF parallel manipulators, *ASME J. Mech. Des.* 124 (2) (2002) 254–258.

- [13] S. Bhattacharyya, H. Hatwal, A. Ghosh, On the optimum design of Stewart platform type parallel manipulators, *Robotica* 13 (2) (1995) 133–140.
- [14] B.S. El-Khasawneh, P.M. Ferreira, Computation of stiffness and stiffness bounds for parallel link manipulators, *Int. J. Mach. Tools Manuf.* 39 (2) (1999) 321–342.
- [15] X.-J. Liu, Z.-L. Jin, F. Gao, Optimum design of 3-DOF spherical parallel manipulators with respect to the conditioning and stiffness indices, *Mech. Mach. Theory* 35 (9) (2000) 1257–1267.
- [16] H. Lipkin, J. Duffy, Hybrid twist and wrench control for a robotic manipulator, *ASME J. Mech. Transm. Autom. Des.* 110 (1988) 138–144.
- [17] S. Huang, J.M. Schimmels, The eigenscrew decomposition of spatial stiffness matrix, *IEEE Trans. Robot. Autom.* 16 (2) (2000) 146–156.
- [18] T. Patterson, H. Lipkin, A classification of robot compliance, *ASME J. Mech. Des.* 115 (3) (1993) 581–584.
- [19] Y. Li, Q. Xu, Kinematics and stiffness analysis for a general 3-PRS spatial parallel mechanism, in: *Proceedings of 15th CISM-IFTOMM Symposium on Robot Design, Dynamics and Control, 2004, Rom04-15*.
- [20] J.-P. Merlet, Solving the forward kinematics of a Gough-type parallel manipulator with interval analysis, *Int. J. Robot. Res.* 23 (3) (2004) 221–235.